



Enhanced Dielectric Loss and Magnetic Loss Properties of Copper Oxide-Nanowire-Covered Carbon Fiber Composites by Porous Nickel Film

Jun Zeng^{1*}, Shiquan Zhang¹, Jun Xue¹, Huili Dai¹, Long Xia², Wenyanhong Cai¹, Yanhua Tang¹ and Chaoyi Xu¹

¹ Department of Basic, Engineering University of PAP, Xi'an, China, ² School of Materials Science and Engineering, Harbin Institute of Technology, Weihai, China

OPEN ACCESS

Edited by:

Biao Zhao,
Zhengzhou University of
Aeronautics, China

Reviewed by:

Qing Da An,
Dalian Polytechnic University, China
Guang-Sheng Wang,
Beihang University, China
Hongjing Wu,
Northwestern Polytechnical
University, China

*Correspondence:

Jun Zeng
zengjun2006@gmail.com

Specialty section:

This article was submitted to
Polymeric and Composite Materials,
a section of the journal
Frontiers in Materials

Received: 19 February 2020

Accepted: 16 April 2020

Published: 29 May 2020

Citation:

Zeng J, Zhang S, Xue J, Dai H, Xia L,
Cai W, Tang Y and Xu C (2020)
Enhanced Dielectric Loss and
Magnetic Loss Properties of Copper
Oxide-Nanowire-Covered Carbon
Fiber Composites by Porous Nickel
Film. *Front. Mater.* 7:123.
doi: 10.3389/fmats.2020.00123

A porous nickel film of agglomerated nanoparticles, 1.5–2.0 μm in thickness, was used to enhance the microwave absorption and ferromagnetic properties of nanowire-like copper oxide-covered carbon fiber composites. Firstly, the porous nickel film/carbon fiber composites were prepared by a plating route, using a current intensity of 120 mA for 30 min (sample S1) or 40 min (sample S2), respectively. Then, the copper oxide/porous nickel/carbon fiber composites (CNCF1 and CNCF2) were synthesized by electroless copper deposition and thermal oxidation (for sample S1 and sample S2). The microwave absorption properties of the composites were investigated over the frequency range 1–18 GHz. The results showed that the strongest reflectivity loss (RL) values of CuO/carbon fiber (CCF) and of CNCF1-2 composites were –25.93 dB at 3.59 GHz with a matching layer thickness of 2.4 mm, –27.87 dB at 6.67 GHz with a matching layer thickness of 2.5 mm, and –54.82 dB at 9.23 GHz with a matching layer thickness of 2.192 mm. When the RL values of CCF and CNCF1-2 composites were lower than –10 dB, the absorption frequency ranged from 8.12 to 9.64 GHz (1.52 GHz in absorption bandwidth, 1.5 mm in thickness), 6.45 to 8.81 GHz (2.36 GHz in absorption bandwidth, 2.4 mm in thickness), and 10.51 to 14.35 GHz (3.84 GHz in absorption bandwidth, 1.8 mm in thickness), respectively. Therefore, the CNCF2 composites showed the best microwave absorption properties and are potential microwave absorption candidates, offering thinness, strong absorption, and wide frequency.

Keywords: microwave absorption properties, copper oxide, porous nickel, absorption bandwidth, carbon fiber

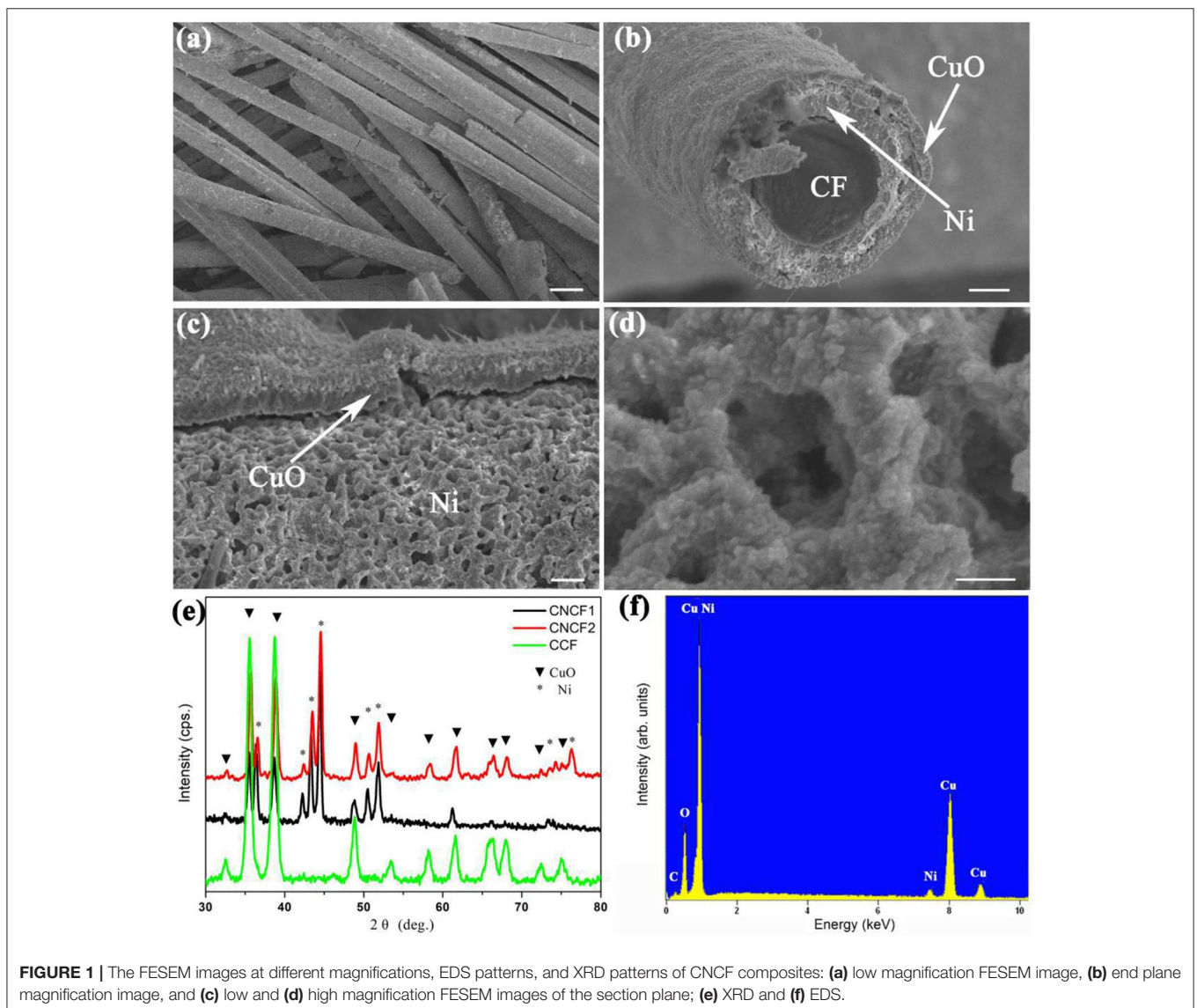
INTRODUCTION

In recent years, the rapid increase in high-frequency circuit devices, electronic systems, and military instruments using electromagnetic waves in the gigahertz (GHz) range has led to a serious problem of electromagnetic interference (EMI). In order to solve the EMI problem and improve application, wide frequency range, low-density, thin, strongly absorbing, and effective microwave absorption materials have attracted significant attention (Yusoff et al., 2002; Ramprasad et al., 2004; Lakshmi et al., 2009). Over the past decade, a variety of materials have been made to develop desirable

microwave-absorbing materials. For example, ferrites (Gao et al., 2019) and composites (Dong et al., 2008; Shah et al., 2015; Yang et al., 2017) have been used as microwave absorbers due to their properties of strong absorption by magnetic loss or dielectric loss. However, the relatively narrow absorption frequency range of these microwave absorbers is limiting their practical applications in the military field.

Recently, because of its excellent magnetic and microwave-absorbing properties, nickel (Ni), hollow or porous materials, has been extensively investigated. Wang et al. (2013) reported that hollow nickel spheres prepared with electroless deposition and template corrosion methods showed excellent microwave absorption properties. The result showed the sphere's shell thickness was an important factor for the microwave absorption properties. Zhu et al. (2015) the use of microwave-assisted synthesis of graphene-Ni composites to enhance microwave absorption properties in the Ku-band. Zhang et al. (2019)

reported that thistle-like CoNi with dielectric Ag-decorated graphene composites synthesized by a facile two-step strategy could be used as high-performance microwave absorbing materials. Li et al. (2009) reported the use of Co-P-coated hollow nickel spheres prepared by the electroless deposition method as microwave absorbers. Lan et al. (2020) reported that $\text{Co}_{1.29}\text{Ni}_{1.71}\text{O}_4$ hollowed-out spheres synthesized with a hydrothermal method had high-efficiency EM wave absorption properties. Liu et al. (2011) reported on the preparation of rod-shaped Co-Ni-P shells by metallizing Bacillus to make microwave absorbing materials. The rod-shaped Co-Ni-P shells exhibited excellent microwave absorption properties, with a microwave absorption frequency range from 5 to 17 GHz. Lan et al. (2015) reported that coating flake-shaped diatomite with Ni-Fe alloy by electroplating gave it excellent electromagnetic properties. Therefore, in this work, multi-layer copper oxide/porous nickel/carbon fiber (CNCF) composites were



successfully prepared with electroless deposition, electroplating, and thermal oxidization methods. The porous nickel and the multi-layer structure were used to enhance the ferromagnetic properties and to enable proper impedance matching of CNCF composites for excellent microwave absorption properties. In order to further study the microwave absorption properties of CNCF composites, the electromagnetic parameters, dielectric loss, and magnetic loss were analyzed, and thin, wide-frequency, and strong microwave absorption materials were obtained.

EXPERIMENTAL SECTION

Materials

In this work, carbon fibers with 3,000 filaments were selected, with the filament diameter being from 7 to 10 μm . The nickel chloride, nickel sulfate, bluestone, and formaldehyde 37% used were analytical reagents available on the market.

Methodology

CNCF composites were prepared by oxidizing Cu-covered Ni/carbon fiber composites in air. Electroless deposition and electroplating were used to synthesize Cu-covered Ni/carbon fiber composites at room temperature, respectively. Before the

surface coating treatment, the carbon fibers were cut to 2–3 mm in length. Firstly, the Ni/carbon fiber composites were prepared with the current intensity at 120 mA for 30 min (S1) and 40 min (S2), respectively. The electroplating Ni bath consisted of 30–40 g/l nickel chloride solution and 170–180 g/l nickel sulfate solution at pH 11–12. Subsequently, the S1 and S2 were washed with distilled water and dried. The Ni/carbon fiber composites were electrolessly plated with copper for 1 h at room temperature, for which the bath consisted of 10–30 ml/l formaldehyde solution and 8–20 g/l bluestone at pH 12–13. After being dried in air, they were oxidized at 400°C for 4 h in air. After cooling down naturally to room temperature, CNCF1 and CNCF2 composites were obtained, respectively.

Characterization

X-ray diffraction (XRD, Philips X' per pro) was used to investigate the structure of the sample. The composition and surface morphology of CNCF composites were analyzed by energy dispersive spectrometer (EDS, Thermo Electron Corporation) and field emission scanning electron microscope (FESEM, Hitachi S4800). Cu K_{α} radiation (45 kV and 40 mA) was used for XRD measurements. The pioneer detector was used to gather EDS spectra with a 20.0 keV accelerating voltage and 89.8 deg takeoff angle. A vector network analyzer (Agilent E8363B

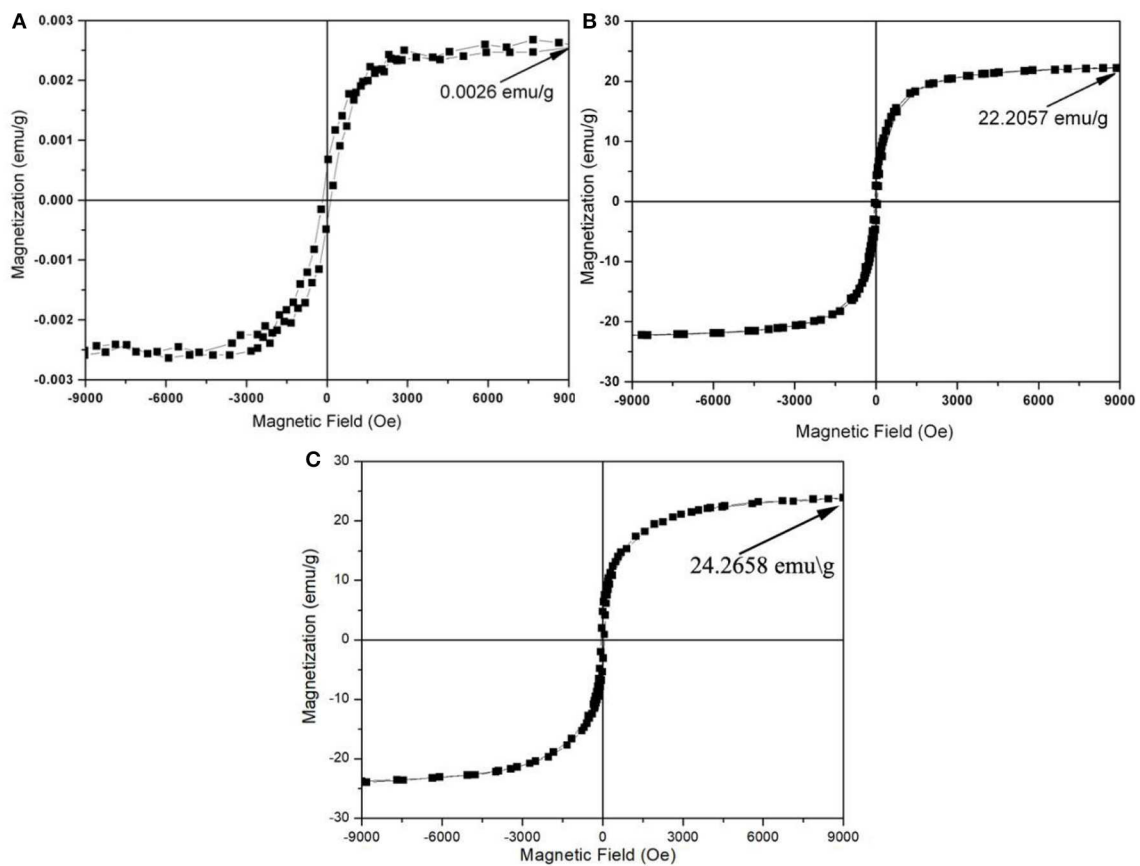


FIGURE 2 | Hysteresis loops of samples: **(A)** CCF, **(B)** CNCF1, and **(C)** CNCF2 composites.

PNA) was used to analyze the complex permittivity ($\epsilon_r = \epsilon' - j\epsilon''$) and complex permeability ($\mu_r = \mu' - j\mu''$) of CuO/CF (CCF) and CNCF composites by the coaxial line method. The frequency covered 1–18 GHz. The samples were prepared to form a ring (7 mm in external diameter, 3 mm in internal diameter), which consisted of composites (30 wt %) and paraffin (70 wt %). Finally, the composite reflectivity loss (RL) was calculated by Equations (1) and (2):

$$Z_{in} = (\mu_r/\epsilon_r)^{1/2} \tanh[j(2\pi fd/c)(\mu_r\epsilon_r)^{1/2}] \quad (1)$$

$$RL(dB) = 20 \log_{10} |(Z_{in} - Z_0)/(Z_{in} + Z_0)| \quad (2)$$

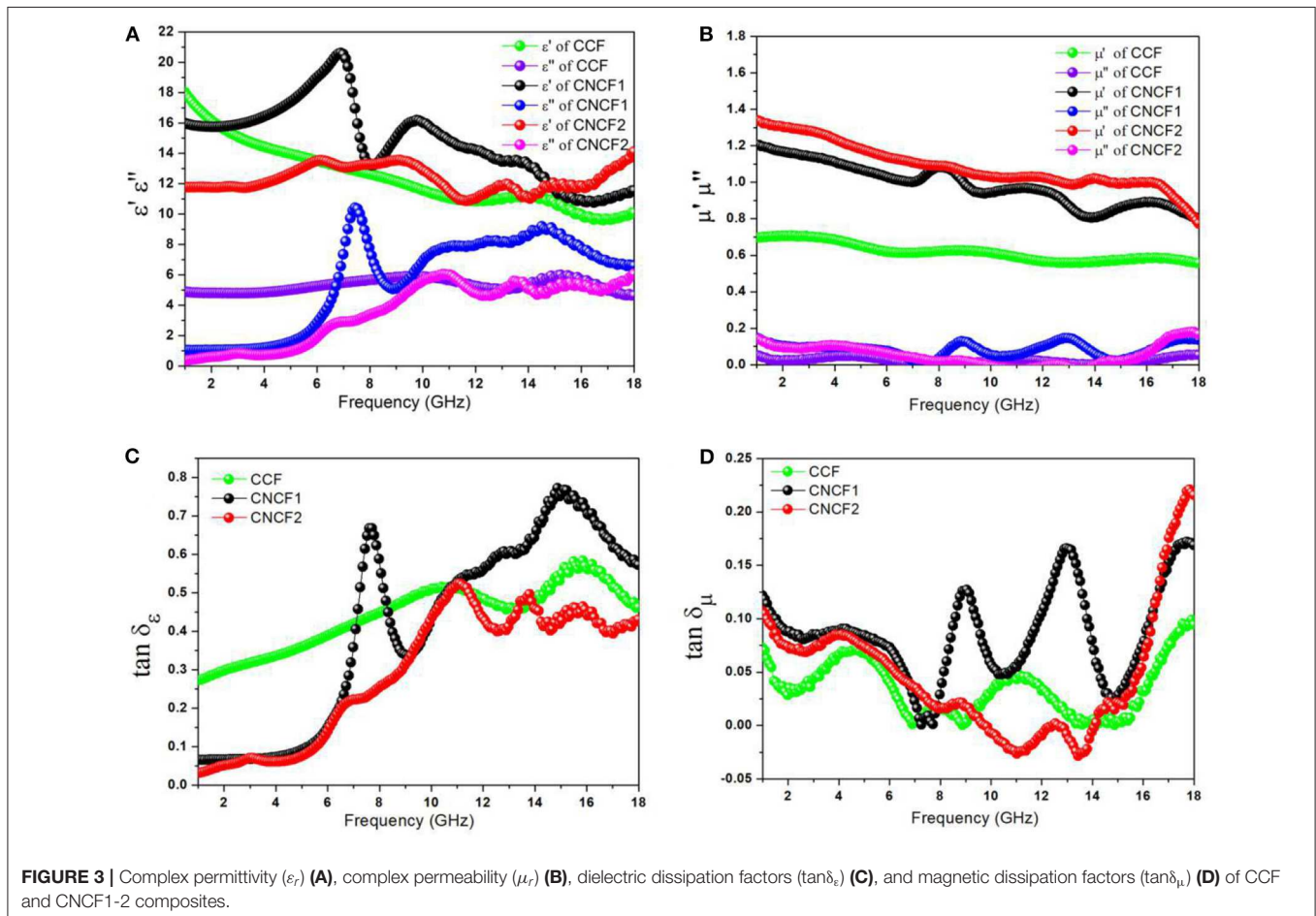
where Z_{in} is the microwave absorption material input impedance and Z_0 is the air impedance, f is the microwave frequency, and d and c are the thickness of the microwave absorbing material and the velocity of light, respectively. The microwave absorption rate of samples reaches 68 and 90% on the basis of Equations (1) and (2), when the RL value is -5 and -10 dB.

RESULTS AND DISCUSSION

Figure 1 shows the morphology at different magnifications, EDS spectrum, and XRD pattern of CNCF1 composites. It was

found that all of the fibers were coated with copper oxide (**Figure 1a**). The end-plane magnification image of CNCF1 composites showed that the components of the materials were carbon fiber (CF, 7–10 μm in diameter), a nickel film layer (Ni, 1.5–2.0 μm in thickness), and copper oxide film (CuO, 1.0–1.5 μm in thickness) (**Figure 1b**). **Figures 1c,d** represent FESEM images of the section plane for CNCF1 composites at different magnifications. Large numbers of agglomerated grains and a 50 nm–1 μm porous structure are shown in the Ni film layer. **Figure 1e** shows the XRD patterns of CCF and CNCF1-2 composites. The results show that the composites consisted of face-centered-cubic Ni, monoclinic CuO films, and carbon fibers, respectively. In previous work (Zeng et al., 2009a,b), the preparation of CuO nanowires/carbon fiber composites by electroless deposition and thermal oxidation was proved by TEM. Additionally, the EDS spectrum of the sample (**Figure 1f**) showed that the microwave absorption materials consist of the four elements, Ni, C, O, and Cu. Therefore, according to the results of the FESEM, XRD pattern, and EDS spectrum, CNCF composites with a multi-layer structure had been obtained.

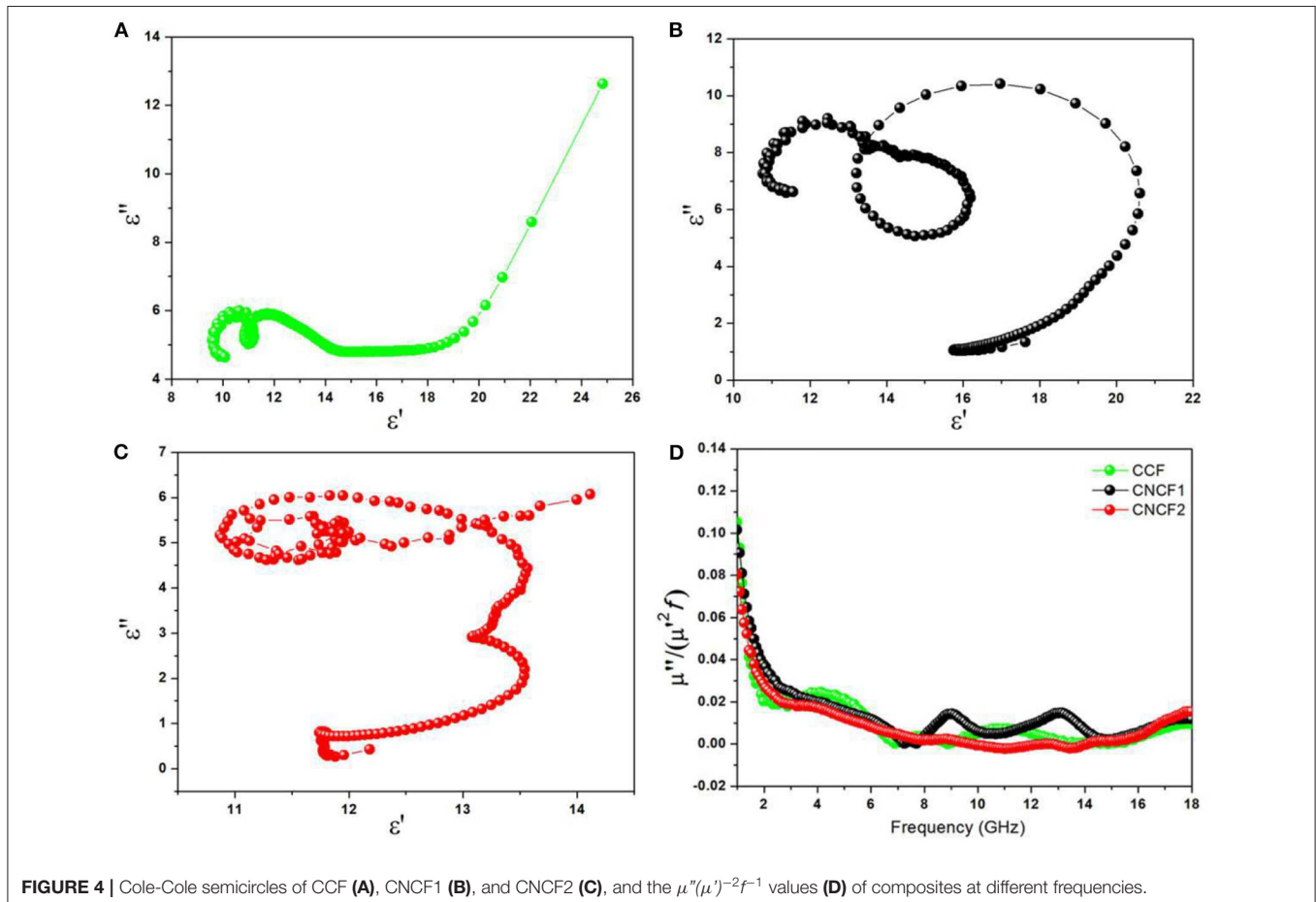
In the interest of analyzing the magnetic property of CCF composites, the hysteresis loops of CCF, CNCF1, and CNCF2 composites were characterized by using a vibrating sample magnetometer (VSM) at room temperature (**Figure 2**).



The saturation magnetization values of CCF composites, CNCF1 composites, and CNCF2 composites were 0.0026, 22.2057, and 24.2658 emu/g at an external field of 9×10^3 Oe, respectively. The magnetic property of CNCF composites was enhanced with an increase in the thickness of the porous Ni film. Therefore, the magnetic property of CNCF composites was enhanced mainly by the porous Ni. In our previous work (Zeng et al., 2009c), we found that defects such as oxygen vacancies resulted in the magnetic property of CCF composites. In previous reports (Jia et al., 2008; Kang et al., 2010; Sun et al., 2013; Wang et al., 2013; Lan et al., 2020), Ni presented excellent ferromagnetic behavior. According to electromagnetic complementary theory, Ni is propitious for improving microwave absorption properties.

Generally, microwave absorption properties are strongly associated with permeability. ϵ' or μ' represent the storage ability of electrical/magnetic energy, and ϵ'' or μ'' mean the dissipation ability (Wang et al., 2019; Wu et al., 2020a). In order to further study the microwave absorption properties of the composites, the dielectric dissipation factors ($\tan\delta_\epsilon = \epsilon''/\epsilon'$) and the magnetic dissipation factors ($\tan\delta_\mu = \mu''/\mu'$) were analyzed on the basis of the permeability and the permittivity, respectively. **Figure 3** shows the ϵ_r , μ_r , $\tan\delta_\mu$ and $\tan\delta_\epsilon$ values of composites with increasing frequency from 1 to 18 GHz. The results show that the ϵ'' and ϵ' values of CCF composites were stable and quickly

reducing, respectively, producing two relatively smooth curves. The ϵ'' and ϵ' values of CNCF1 composites showed two wide peaks (for ϵ'' , in the frequency ranges 2.61–8.87 and 8.87–17.73 GHz; for ϵ' , in the frequency ranges 1.98–8.24 GHz and 8.24–16.48 GHz). The ϵ'' and ϵ' values of CNCF2 composites showed a wide peak (for ϵ'' , in the frequency range 4.31–18 GHz) and two wide peaks (for ϵ' , in the frequency ranges 2.61–8.87 GHz and 8.87–17.73 GHz), respectively (**Figure 3A**). The CNCF1-2 composites showed higher ϵ'' values, indicating that the dielectric losses of CNCF1-2 composites were more substantial than that of CCF composites. The $\tan\delta_\epsilon$ of CNCF and CCF composites increased from 0.07 to 0.77 and 0.27 to 0.57, respectively, and showed two peaks (**Figure 3C**). The $\tan\delta_\epsilon$ of CNCF1-2 composites exhibited much sharper correlation and better discrimination peaks than that of the CCF composites, indicating that the dielectric energy storage and dielectric loss ability of CNCF1-2 composites were enhanced by the porous Ni. Usually, dielectric loss is related to interfacial polarization, dipole polarization, and conduction loss (Khani et al., 2016; Wu et al., 2020b). In this work, the porous structures and multiple interfaces of CNCF1-2 composites lead to abundant oxygen vacancies, lattice defects, and interfaces, enhancing the dipole polarization and displacement polarization effect. The polarizations can be further confirmed on the basis of the



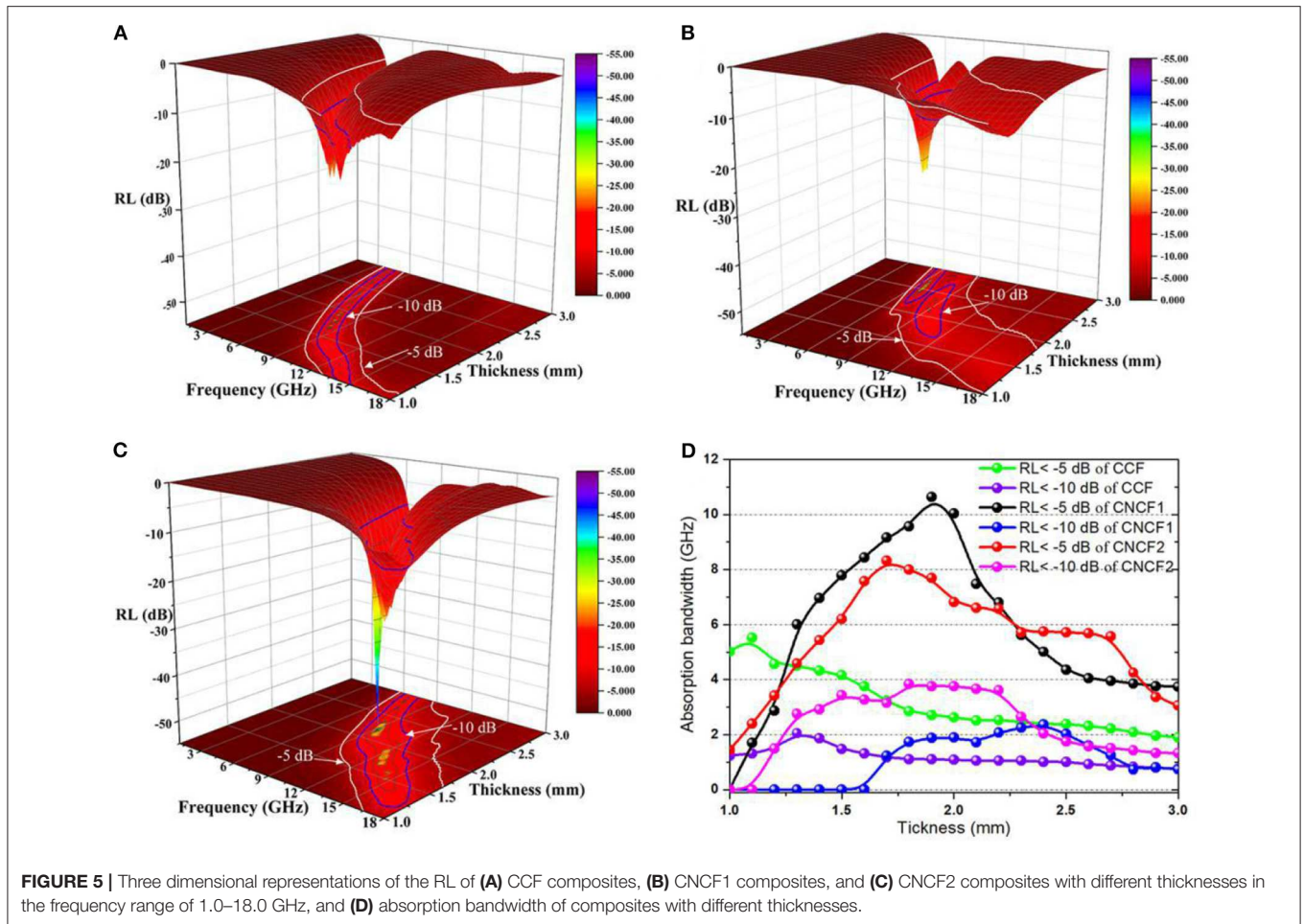


FIGURE 5 | Three dimensional representations of the RL of (A) CCF composites, (B) CNCF1 composites, and (C) CNCF2 composites with different thicknesses in the frequency range of 1.0–18.0 GHz, and (D) absorption bandwidth of composites with different thicknesses.

Cole-Cole semicircles shown in **Figures 4A–C**. The CNCF2 composites shown more semicircles than do the CCF and CNCF1 composites, indicating better microwave absorption properties.

As is well-known, exchange resonance contributes to high-frequency peaks above 10 GHz, and natural ferromagnetic resonance contributes to low-frequency peaks under 10 GHz. The μ' values of CCF and CNCF1-2 composites show slow downtrends from 0.70 to 0.50, 1.20 to 0.80, and 1.34 to 0.77, respectively. The μ'' values of CCF and CNCF1-2 composites decreased and then increased with an increase in frequency, and both the μ'' and μ' values of CNCF1-2 composites were better than those of CCF composites. For the CCF composites, both the μ'' and μ' of the permeability were almost invariable. However, both the μ'' and μ' of the CNCF1 composites showed three wide peaks (for μ'' , in the frequency ranges 7.26–10.39 GHz, 10.39–14.87 GHz, and 14.87–18.00 GHz; for μ' , in the frequency ranges 6.99–9.77 GHz, 9.77–13.88 GHz, and 13.88–18.00 GHz). The μ'' of the CNCF2 composites showed two wide peaks at 1–11 and 11–18 GHz. **Figure 3D** shows that the $\tan\delta_\mu$ of CCF and CNCF1-2 increased from 0 to 0.10, 0.01 to 0.17, and 0 to 0.18, respectively. Comparing with the $\tan\delta_\mu$ of CCF composites, both the CNCF1 and the CNCF2 composites showed five

stronger and broader resonance peaks, which implied that the strong microwave absorption of the composites occurred due to exchange resonance and natural ferromagnetic resonance (Zhang et al., 2006; Dong et al., 2008; Lan et al., 2020). Additionally, if $C_0 = \mu''/(\mu'^2 f)$ is constant with an increase in frequency, eddy current loss is the main contribution to magnetic loss (Xie et al., 2013). The C_0 value of the three samples shown five obvious peaks, indicating that eddy current loss was eliminated (**Figure 4D**). The natural resonance was representative of strong magnetic loss abilities, indicating that the microwave absorption properties had been promoted. Therefore, the CNCF1-2 composites showed stronger dielectric loss and magnetic loss in the electromagnetic field than the CCF composites, indicating that both the magnetic loss and dielectric loss enhanced the microwave absorption property of CNCF1-2 composites.

The three-dimensional representations of RL (**Figures 5A–C**) showed the theoretical RL of the CCF and CNCF1-2 composites in the 1–18 GHz range, when the thickness covered 1.0 to 3.0 mm. It can be found that the microwave absorption properties and RL peaks can be controlled by controlling the thickness of the microwave absorbing materials. For the CNCF composites, there is a stronger peak and wider absorption frequency than for CCF

composites. **Figure 5D** shows the absorption bandwidth of CCF and CNCF1-2 composites with increasing thickness from 1 to 3 mm. The absorption bandwidths of CCF composites (RL <-10 dB and RL <-5 dB) slowly decreased with the increase in sample thickness and showed a sharp peak, and the widest absorption bandwidths were at 1.52 GHz (RL <-10 dB, 1.50 in thickness) and 5.64 GHz (RL <-5 dB, 1.05 in thickness), respectively. As for the CNCF1-2 composites, the absorption bandwidths (RL <-10 dB and RL <-5 dB) increased to a maximum and then decreased with increase in the thickness of the microwave absorber. In particular, the widest absorption bandwidths were at 2.36 GHz (RL <-10 dB, 2.40 in thickness) and 10.39 GHz (RL <-5 dB, 1.925

in thickness) and at 3.84 GHz (RL <-10 dB, 1.80 in thickness) and 8.32 GHz (RL <-5 dB, 1.70 in thickness), respectively, and they were wider than those of CCF composites. Therefore, the bandwidth absorption of composites may be enhanced by the porous nickel.

Figure 6 presents the RL and the strongest RL of CCF and CNCF1-2 composites vs. change in thickness in the frequency range of 1–18 GHz. It can be found that the strongest RL values of CCF composites presented two peaks with different thickness and that the optimal RL value was -23.12 dB at 8.24 GHz for a thickness of 1.7 mm (**Figures 6A,D**). As to the CNCF1-2 composites, the strongest RL values first decreased and then

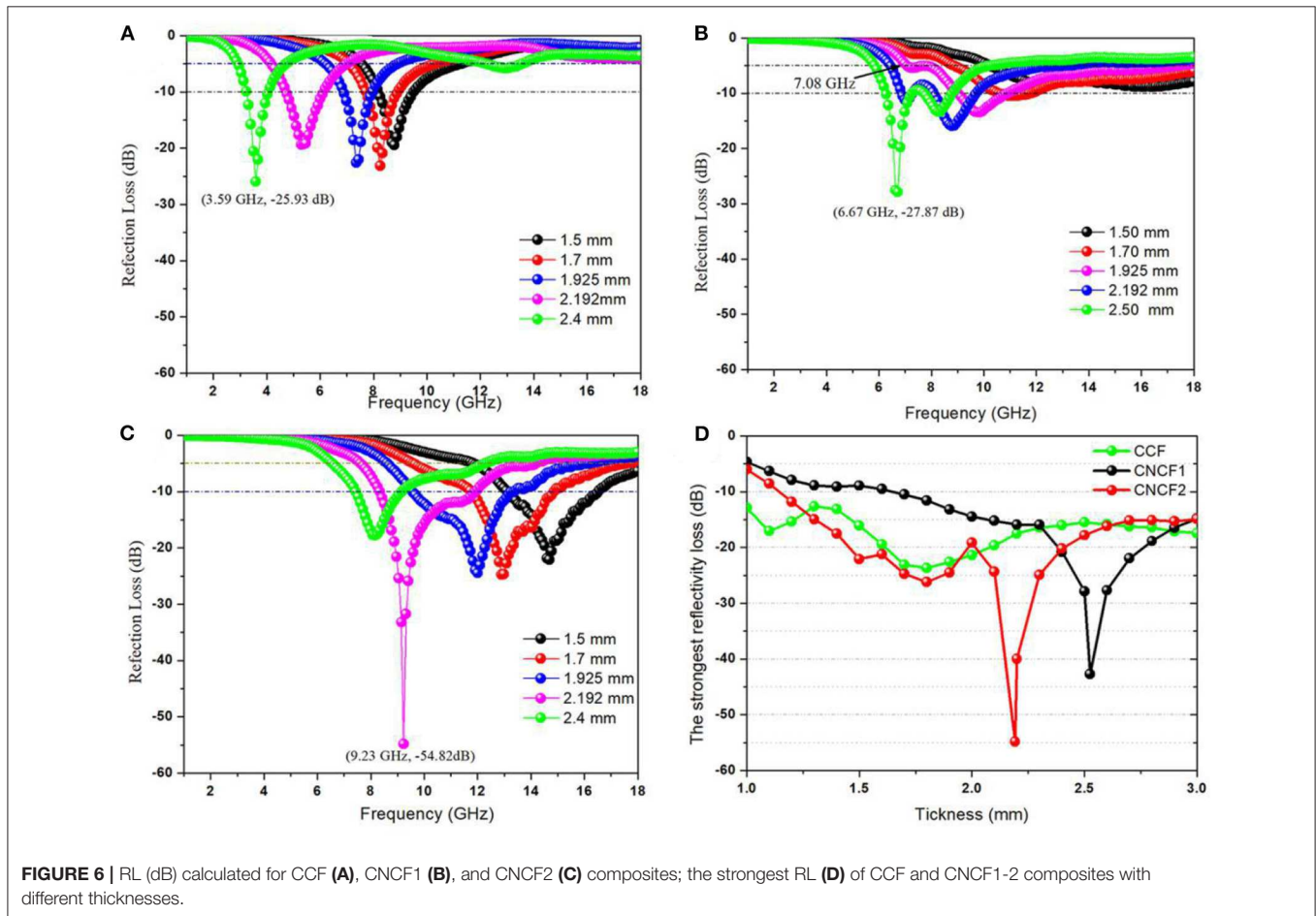


TABLE 1 | The best absorption bandwidths and corresponding parameters for CNCF composites vs. previously reported absorbers.

Materials	Bandwidth (RL <-10 dB, GHz)	Optimum Thickness (mm)	Strongest RL (dB)	f of the strongest RL (GHz)
Graphene@Ni@C (Li et al., 2015)	3.20	1.6	-34.2	13.9
Ni-Co nanoferrites (Chen et al., 2015)	3.60	3.0	-36.2	11.52
CoNi-CuO (Gao et al., 2017)	3.4	2.5	-25.1	13.2
Ni-carbon nanofibers (Shen et al., 2018)	3.0	3.0	-44.9	8.4
CCF composites (this work)	1.52	1.5	-23.12	8.24
CNCF1 composites (this work)	2.36	2.4	-27.87	6.67
CNCF2 composites (this work)	3.84	1.8	-54.82	9.23

increased as the thickness increased, and the optimal RL value was much more promoted to -27.87 dB at 6.67 GHz for the thickness of 2.5 mm, and -54.82 at 9.23 GHz for the thickness of 2.192 mm (Figures 6B–D). Therefore, the CNCF1-2 composites shown stronger absorption properties than the CCF composites. Both magnetic loss and dielectric loss were major contributions to the microwave absorption properties. The magnetic loss of microwave absorption materials has been related to the eddy current effect, domain-wall resonance, magnetic hysteresis, natural resonance, and exchange resonance (Ma et al., 2012; Ding et al., 2017; Wei et al., 2019) and the dielectric loss is thought to be rooted in the interfacial polarization, ion polarization, electron polarization, etc. (Watts et al., 2003). For the CCF composite, in previous work, we thought that the interfacial electric polarization contributed to the microwave absorption properties (Zeng et al., 2009c). In another previous report, hollow or porous structures presented excellent microwave absorption properties, such as porous $\text{Fe}_3\text{O}_4/\text{CuI}/\text{PANi}$ nanosheets (Liu et al., 2014), hollow-porous carbon fiber composites (Xie et al., 2009), and hollow nickel spheres (Wang et al., 2013). In this work, the porous Ni of the CCF composites resulted in charge multipoles at the interfaces of the composites. The multiple interfaces such as between porous Ni and carbon fibers, cupric oxide nanostructures and porous Ni, nanostructures and air bubbles, and cupric oxide nanostructures and paraffin, could be propitious for enhancing the microwave absorption properties in a high-frequency electromagnetic field. In addition, the porous Ni film in the multilayer composites promoted their magnetic and electric properties. The $\tan\delta_\mu$ of CNCF1-2 composites was higher than that of the CCF composites and exhibited much sharper correlations and better discrimination peaks (Figure 3D). For the magnetic materials (Ni), natural resonance, exchange resonance, domain wall resonance, and dimensional resonance were related to strong magnetic loss properties (Aharoni, 1991; Zhang et al., 2006; Dong et al., 2008; Li et al., 2009). The porous Ni was beneficial for enhancing microwave absorption. Compared with some reported core-shell samples and typical Ni-based composites in previous reports (Chen et al., 2015; Li et al., 2015; Gao et al., 2017; Shen et al., 2018), the CNCF2 composites exhibited excellent microwave absorption properties (Table 1). Therefore, the CNCF composites are potential candidates for

making thin, strongly absorbing, and wide-frequency microwave absorption material.

CONCLUSIONS

In this work, porous Ni with agglomerated nanoparticles was used to enhance the ferromagnetic and microwave absorption properties of CCF composites. The optimal RL value of the CNCF2 composite was the most promoted to -54.82 dB at 9.23 GHz with a thickness of 2.192 mm. The widest absorption bandwidths were 8.32 GHz (9.58–17.9 GHz, 1.7 mm in thickness) and 3.84 GHz (10.51–14.35 GHz, 1.8 in thickness) when the RL values of the CNCF composites were <-5 and -10 dB, respectively. In particular, all of the microwave absorption parameters of CNCF composites were better than those of CCF composites; this was attributed to the porous Ni introduced between the CuO film and carbon fibers. Therefore, CNCF composites showed excellent magnetic loss and microwave absorption properties in a high-frequency electromagnetic field. It is believed that the CNCF composites are potential candidates for making a thin, strongly absorbing, and wide-frequency microwave absorption material.

DATA AVAILABILITY STATEMENT

The original contributions presented in the study are included in the article/supplementary materials; further inquiries can be directed to the corresponding author.

AUTHOR CONTRIBUTIONS

All authors listed have made a substantial, direct and intellectual contribution to the work, and approved it for publication.

FUNDING

This work was supported by the National Natural Science Foundation of China (51302318), the Province Natural Science Foundation of Shan Xi (2019JM-317, 2011JQ6013), and the Nano-Microwave Absorbent Materials Innovative Research Team of the Engineering University of PAP.

REFERENCES

- Aharoni, A. (1991). Exchange resonance modes in a ferromagnetic sphere. *J. Appl. Phys.* 69:7762. doi: 10.1063/1.347502
- Chen, B. Y., Chen, D., Kang, Z. T., and Zhang, Y. Z. (2015). Preparation and microwave absorption properties of Ni-Co nanoferrites. *J. Alloys Compd.* 618, 222–226. doi: 10.1016/j.jallcom.2014.08.195
- Ding, D., Wang, Y., Li, X. D., Qiang, R., Xu, P., Chu, W. L., et al. (2017). Rational design of core-shell Co@C microspheres for high-performance microwave absorption. *Carbon* 111, 722–732. doi: 10.1016/j.carbon.2016.10.059
- Dong, X. L., Zhang, X. F., Huang, H., and Zuo, F. (2008). Enhanced microwave absorption in Ni/polyaniline nanocomposites by dual dielectric relaxations. *Appl. Phys. Lett.* 92:013127. doi: 10.1063/1.2830995
- Gao, S., Zhou, N., An, Q., Xiao, Z., Zhai, S., and Shi, Z. (2017). Facile solvothermal synthesis of novel heterostructured CoNi–CuO composites with excellent microwave absorption performance. *RSC Adv.* 7:43689. doi: 10.1039/C7RA07353D
- Gao, X., Wang, Y., Wang, Q. G., Wu, X. M., Zhang, W. Z., Zong, M., et al. (2019). Facile synthesis of a novel flower-like BiFeO₃ microspheres/graphene with superior electromagnetic wave absorption performances. *Ceram. Int.* 45, 3325–3332. doi: 10.1016/j.ceramint.2018.10.243
- Jia, F., Zhang, L., Shang, X., and Yang, Y. (2008). Non-aqueous sol-gel approach towards the controllable synthesis of nickel nanospheres, nanowires, and nanoflowers. *Adv. Mater.* 20, 1050–1054. doi: 10.1002/adma.200702159
- Kang, Y. Q., Cao, M. S., Yuan, J., Zhang, L., Wen, B., and Fang, X. Y. (2010). Preparation and microwave absorption properties of basalt fiber/nickel core-shell heterostructures. *J. Alloys Compd.* 495, 254–259. doi: 10.1016/j.jallcom.2010.01.143
- Khani, O., Shoushtari, M. Z., Jazirehpour, M., and Shams, M. H. (2016). Effect of carbon shell thickness on the microwave absorption of

- magnetite-carbon core-shell nanoparticles. *Ceram. Int.* 42, 14548–14556. doi: 10.1016/j.ceramint.2016.06.069
- Lakshmi, K., John, H., Mathew, K. T., Joseph, R., and George, K. E. (2009). Microwave absorption, reflection and EMI shielding of PU-PANI composite. *Acta. Mater.* 57, 371–375. doi: 10.1016/j.actamat.2008.09.018
- Lan, D., Qin, M., Liu, J., Wu, G., Zhang, Y., and Wu, H. (2020). Novel binary cobalt nickel oxide hollowed-out spheres for electromagnetic absorption applications. *Chem. Eng. J.* 382:122797. doi: 10.1016/j.cej.2019.122797
- Lan, M., Li, H., Huang, W., Xu, G., and Li, Y. (2015). Effect of cathode vibration and heat treatment on electromagnetic properties of flake-shaped diatomite coated with Ni-Fe alloy by electroplating. *J. Magn. Magn. Mater.* 377, 243–251. doi: 10.1016/j.jmmm.2014.10.131
- Li, C., Huang, Y., and Chen, J. (2015). Dopamine-assisted one-pot synthesis of graphene@Ni@C composites and their enhanced microwave absorption performance. *Mater. Lett.* 154, 136–139. doi: 10.1016/j.matlet.2015.04.076
- Li, Z., Shen, B., Deng, Y., Liu, L., and Hu, W. (2009). Preparation and microwave absorption properties of electroless Co-P-coated nickel hollow spheres. *Appl. Surf. Sci.* 255, 4542–4546. doi: 10.1016/j.apsusc.2008.11.066
- Liu, J., Zhang, X., Li, S., and Yu, M. (2011). Microwave absorption properties of rod-shaped Co-Ni-P shells prepared by metallizing bacillus. *Appl. Surf. Sci.* 257, 2383–2386. doi: 10.1016/j.apsusc.2010.09.107
- Liu, L., Zhang, H., Li, J., Shen, Y., Wang, C., Qiu, L., et al. (2014). Porous Fe₃O₄/CuI/PANI nanosheets with excellent microwave absorption and hydrophobic property. *Mater. Res. Bull.* 53, 58–64. doi: 10.1016/j.materresbull.2014.02.001
- Ma, Z., Liu, Q. F., Yuan, J., Wang, Z. K., Cao, C. T., and Wang, J. B. (2012). Analyses on multiple resonance behaviors and microwave reflection loss in magnetic Co microflowers. *Phys. Status Solidi. B* 249, 575–580. doi: 10.1002/pssb.201147382
- Ramprasad, R., Zurcher, P., Petras, M., Miller, M., and Renaud, P. (2004). Magnetic properties of metallic ferromagnetic nanoparticle composites. *J. Appl. Phys.* 96:519. doi: 10.1063/1.1759073
- Shah, A., Wang, Y. H., Huang, H., Zhang, L., Wang, D. X., Zhou, L., et al. (2015). Microwave absorption and flexural properties of Fe nanoparticle/carbon fiber/epoxy resin composite plates. *Compos. Struct.* 131, 1132–1141. doi: 10.1016/j.compstruct.2015.05.054
- Shen, Y., Wei, Y., Ma, J., Li, Q., Li, J., Shao, W., et al. (2018). Tunable microwave absorption properties of nickel-carbon nanofibers prepared by electrospinning. *Ceram. Int.* 45, 3313–3324. doi: 10.1016/j.ceramint.2018.10.242
- Sun, X., He, J. P., Li, G. X., Tang, J., Wang, T., Guo, Y. X., et al. (2013). Laminated magnetic graphene with enhanced electromagnetic wave absorption properties. *J. Mater. Chem. C* 1, 765–777. doi: 10.1039/C2TC00159D
- Wang, G., Wang, L., Gan, Y., and Lu, W. (2013). Fabrication and microwave properties of hollow nickel spheres prepared by electroless plating and template corrosion method. *Appl. Surf. Sci.* 276, 744–749. doi: 10.1016/j.apsusc.2013.03.162
- Wang, L., Wen, B., Bai, X., Liu, C., and Yang, H. (2019). Facile and green approach to the synthesis of zeolitic imidazolate framework nanosheet-derived 2D Co/C composites for a lightweight and highly efficient microwave absorber. *J. Colloid Interf. Sci.* 540, 30–38. doi: 10.1016/j.jcis.2018.12.111
- Watts, P. C. P., Hsu, W. K., Barnes, A., and Chambers, B. (2003). High permittivity from defective multiwalled carbon nanotubes in the X-band. *Adv. Mater.* 15, 600–603. doi: 10.1002/adma.200304485
- Wei, G. K., Wang, T., Zhang, H., Liu, X. T., Han, Y. L., Chang, Y. C., et al. (2019). Enhanced microwave absorption of barium cobalt hexaferrite composite with improved bandwidth via c-plane alignment. *J. Magn. Magn. Mater.* 471, 267–273. doi: 10.1016/j.jmmm.2018.09.063
- Wu, H., Liu, J., Liang, H., and Zang, D. (2020a). Sandwich-like Fe₃O₄/Fe₃S₄ composites for electromagnetic wave absorption. *Chem. Eng. J.* 393:124743. doi: 10.1016/j.cej.2020.124743
- Wu, H., Qin, M., and Zhang, L. (2020b). NiCo₂O₄ constructed by different dimensions of building blocks with superior electromagnetic wave absorption performance. *Compos. Part B Eng.* 182:107620. doi: 10.1016/j.compositesb.2019.107620
- Xie, S., Guo, X. N., Jin, G. Q., and Guo, X. Y. (2013). Carbon coated Co-SiC nanocomposite with high-performance microwave absorption. *Phys. Chem. Chem. Phys.* 15:16104. doi: 10.1039/c3cp52735b
- Xie, W., Cheng, H. F., Chu, Z. Y., Zhou, Y. J., Liu, H. T., and Chen, Z. H. (2009). Effect of FSS on microwave absorbing properties of hollow-porous carbon fiber composites. *Mater. Des.* 30, 1201–1204. doi: 10.1016/j.matdes.2008.06.018
- Yang, R. L., Wang, B. C., Xiang, J. Y., Mu, C. P., Zhang, C., Wen, F. S., et al. (2017). Fabrication of NiCo₂-anchored graphene nanosheets by liquid-phase exfoliation for excellent microwave absorbers. *ACS Appl. Mater. Interfaces* 9, 12673–12679. doi: 10.1021/acsami.6b16144
- Yusoff, A. N., Abdullah, M. H., Ahmad, S. H., Jusoh, S. F., Mansor, A. A., and Hamid, S. A. A. (2002). Electromagnetic and absorption properties of some microwave absorbers. *J. Appl. Phys.* 92:876. doi: 10.1063/1.1489092
- Zeng, J., Tao, P., Wang, S., and Xu, J. (2009a). Preparation and study on radar-absorbing materials of cupric oxide-nanowire-covered carbon fibers. *Appl. Surf. Sci.* 255, 4916–4920. doi: 10.1016/j.apsusc.2008.12.036
- Zeng, J., Xu, J., Tao, P., and Hua, W. (2009b). Ferromagnetic and microwave absorption properties of copper oxide-carbon fiber composites. *J. Alloys Compd.* 487, 304–308. doi: 10.1016/j.jallcom.2009.07.112
- Zeng, J., Xu, J., Wang, S., Tao, P., and Hua, W. (2009c). Ferromagnetic behavior of copper oxide-nanowire-covered carbon fibre synthesized by thermal oxidation. *Mater. Charact.* 60, 1068–1070. doi: 10.1016/j.matchar.2009.03.012
- Zhang, N., Huang, Y., Wang, M., Liu, X., and Zong, M. (2019). Design and microwave absorption properties of thistle-like CoNi enveloped in dielectric Ag decorated graphene composites. *J. Colloid Interf. Sci.* 534, 110–121. doi: 10.1016/j.jcis.2018.09.016
- Zhang, X. F., Dong, X. L., Huang, H., Liu, Y. Y., Wang, W. N., Zhu, X. G., et al. (2006). Microwave absorption properties of the carbon-coated nickel nanocapsules. *Appl. Phys. Lett.* 89:053115. doi: 10.1063/1.2236965
- Zhu, Z., Sun, X., Li, G., Xue, H., Guo, H., Fan, X., et al. (2015). Microwave-assisted synthesis of graphene-Ni composites with enhanced microwave absorption properties in Ku-band. *J. Magn. Magn. Mater.* 377, 95–103. doi: 10.1016/j.jmmm.2014.10.079

Conflict of Interest: The authors declare that the research was conducted in the absence of any commercial or financial relationships that could be construed as a potential conflict of interest.

Copyright © 2020 Zeng, Zhang, Xue, Dai, Xia, Cai, Tang and Xu. This is an open-access article distributed under the terms of the Creative Commons Attribution License (CC BY). The use, distribution or reproduction in other forums is permitted, provided the original author(s) and the copyright owner(s) are credited and that the original publication in this journal is cited, in accordance with accepted academic practice. No use, distribution or reproduction is permitted which does not comply with these terms.